Proceedings of the 7th International Symposium on Cavitation
CAV2009 – Paper No. 5
August 17-22, 2009, Ann Arbor, Michigan, USA

Interfacial cavitation nuclei studied by scanning probe microscopy techniques

K. A. Mørch
Department of Physics and
Center of Quantum Protein
Technical University of Denmark
DK-2800 Kgs. Lyngby

ABSTRACT

The new microscopy techniques for studying solid surfaces, scanning tunneling microscopy (STM) and atomic force microscopy (AFM), also offer possibilities of studying gaseous nano-voids at solid-water interfaces, i.e. cavitation nuclei. The use of STM presupposes that both the surface studied and that of the STM-tip allow electrons to be transferred to/from the location of tunneling. To detect surface nano-voids by STM it is therefore necessary that when the submerged STM-tip during scanning of a surface meets a void, the tunneling barrier is smaller along the cavity surface than if the tip moves on along the drained solid surface below the void. Likewise, the use of AFM for void detection presupposes that the liquid-gas interface of a void can supply a detectable force on the AFM-tip. Otherwise, the tip will ignore the void, and only the solid surface below it will be detected. With both techniques it has proved possible to meet the demands for detection of surface nano-voids, and today their existence is well established. However, the results obtained depend on the technique of microscopy chosen, and on how it is applied, which makes the evaluation of such measurements difficult. Therefore, an analysis of the physics related to void detection by the scanning probe microscopy (SPM) techniques is important. The present paper presents this physics on the basis of experimental results obtained with SPM techniques since the early 1990'es.

TECHNIQUES AND ANALYSIS

Scanning tunneling microscopy

Scanning tunneling microscopy [1] was the first of the SPM techniques to be developed, and therefore it was the one first used for comparison of specimen surfaces in air and in water in search of interfacial cavitation nuclei [2,3,4], originally suggested to exist by Harvey [5]. Specimens of gold (Au), vapour-deposited onto a lacquered aluminum substrate, specimen surfaces of titanium nitride (TiN), deposited onto a tungsten (W) substrate, and specimen surfaces of W were studied. It was revealed that in water the specimen surface topographies appeared notably smoother than in air, Figure 1, when scanned with sharp STM tips made from W. This was a first indication that interfacial voids are present in large numbers at fine roughness structures of submerged solid surfaces (lateral dimensions of up to about 200 nm), and that STM could be used to reveal their existence. But how could surface voids be imaged by STM? And, could the voids be observed by other techniques?

Surface imaging by STM is based on a sharp, *conducting* STM tip being scanned along a *conducting* specimen surface at a constant tip-specimen distance s, in vacuum typically less than 1 nm, maintained by keeping a tunneling current I_t of a few nA in the tip-specimen gap constant by moving the tip up

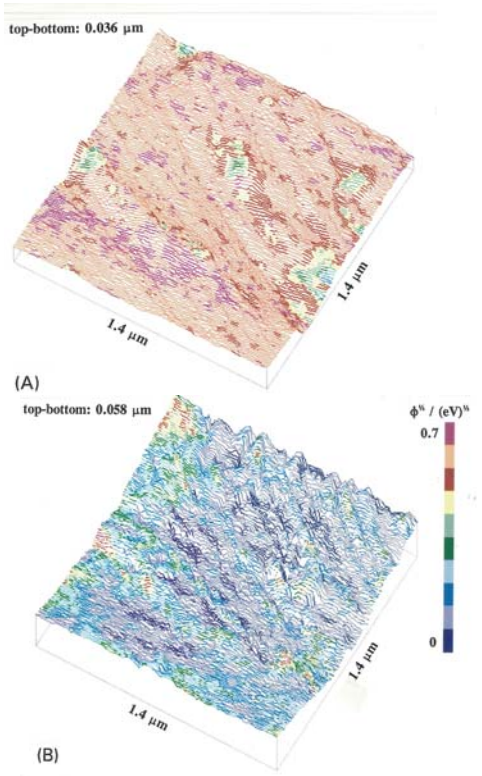

Figure 1. The same element of the surface of a W-specimen recorded with a W-tip (A) when submerged in water, and (B) subsequently in air. We notice the apparent smoothness of the surface in water compared with that in air. Also the tunnelling barrier signal is lower in air than in water because in air the tip is extremely close to the specimen surface, and the thin layers of adsorbed water molecules on their surfaces are in contact. I_t =4 nA [3].

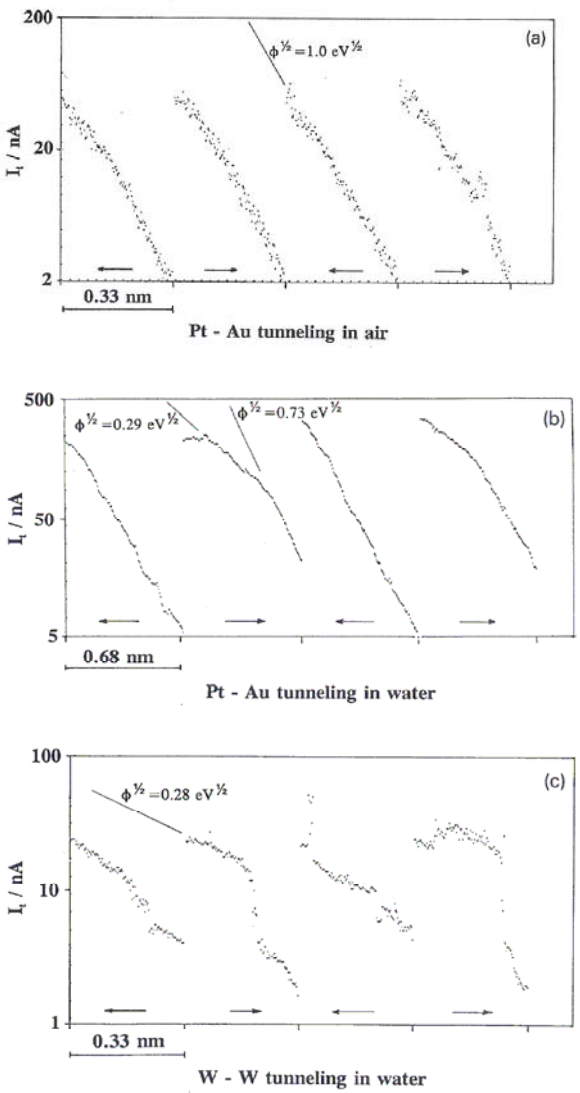

Figure 2. Tunneling current I_t vs. tip-specimen distance s : (a) in air at Pt-Au tunnelling; (b) in water at Pt-Au tunnelling; (c) in water at W-W tunnelling (newly etched specimen). The arrow at each curve shows the direction of tip motion. The tunnelling current feed back loop is activated between each pair of forward and backward tip motion, carried out in 700 ms. In the figures $\Phi^{1/2}$ values corresponding to different line inclinations are shown [3].

and down, following the surface topography during the scanning. In a vacuum gap

$$I_t = I_{t,0} e^{-1.025 s\sqrt{\Phi}} . \qquad (1)$$

Here the mean barrier height Φ (eV) is the mean of the work functions for the tip and specimen materials, typically about 4-5 eV, while s is measured in Å. Thus, I_t is reduced by a factor of ~10 at an increase of s by 1 Å. This sensitivity makes STM capable of ultimately resolving surface structures down to atomic scale. The STM tip is fixed to a piezo-electric scanner which allows fine scale tip motion in the x-, y-, and z-directions, while an inch-worm motor is used for coarse adjustment of the scanner in the z-direction during tip approach when the tunneling current is to be established. During x-y scanning the tunneling barrier can be calculated from tunneling current fluctuations set up by small-amplitude z-vibrations (0.14 nm peak-to-peak amplitude at 1 kHz) of the tip [3].

If STM is used for investigation of solid surfaces in a gas atmosphere, the tunneling barrier is lower than in a vacuum gap - and if used in a liquid, the barrier is even lower. This is apparent from the spectroscopic studies in [3,4], in which the tip was stationary and the feed-back system keeping the tunnelling current constant was de-coupled, thus allowing measurement of the tunneling current I_t vs. the distance s. Here tunnelling barriers of $\Phi \approx 1$ eV in air and $\Phi \approx 0.5$ eV or less in water were obtained by tunneling between platinum and gold. In repeated experiments the $\ln I_t$ vs. s relationships were measured during displacement of the Pt-tip first towards the Au-specimen, then during its retraction, Fig.2a,b. We notice that *in air* $\ln I_t$ vs. s forms single, straight lines, essentially of the same slope at tip approach and retraction, but *in water* only the approach leads to a single, almost straight line, i.e. a single value of the tunneling barrier. At the retraction the line is broken, revealing a notably lower tunneling barrier, $\Phi < 0.1$, as long as the tip and specimen are very near to each other, and even segments of $\Phi \approx 0$ occur. At larger separation the approach and retraction values of the tunneling barriers coincide.

To interpret these results, we focus on the water layers in contact with the solid surfaces of the specimen and the tip, and point out that water molecules in contact with solid surfaces form a solid-like, orderly structured layer, while outside this layer, the water structure soon shifts to the incessantly shifting liquid structure [6], at least at temperatures above 5-10 ^{o}C. In gas, and in particular in water, the width of the tunneling gap is larger than in vacuum, but of the order of a few diameters of the water molecules ($D_{H2O} \approx 0.3$nm) at most. If at spectroscopic tip-specimen approach the orderly structured layers of water on the tip and specimen are squeezed, we can assume that their ordering is broken, making them electronically similar to bulk water, i.e. the tunneling barrier is unaffected during the tip approach. However, at tip retraction the orderly structures are re-established, hereby causing a reduced tunneling barrier until the solid-like water in the interfacial layers on the tip and specimen separate, and the gap again contains water with a fully liquid-like structure. Studies of the electrical properties of orderly structured interfacial water layers are not available. However, these layers seem to hold the key to understanding that actually STM can be used for the recording of surface topography of not only noble metals, but also that of metals with non-conducting surfaces of oxides or coatings, and even of voids located at such surfaces [2,3,4]. The observation of $\Phi \approx 0$ at tip retraction may be due to local detachment of the water from the specimen surface.

The W specimens and tips used for the recordings in Figures 1 and 2c had surfaces covered by WO_2, which has an extremely low conductivity, and this has prevented direct metal–metal tunneling. However, we can imagine that in these experiments charge transfer along the orderly structured interfacial water layers, adsorbed to the extended oxide layers on the tip and specimen, has made the tunneling current I_t possible. This interpretation is supported by the spectroscopic results in Figures 1 and 2c showing tunneling barrier signals of $\Phi \approx 0.4$ eV in water, while remarkably, in atmospheric air values of $\Phi < 0.1$

eV were found. The former value corresponds well to those of Pt-Au tunneling in bulk water, and indicates that at W-W tunneling in water, the tip and specimen have actually been separated by bulk water. Remarkably, in air the tunneling barrier is an order of size smaller at W-W tunneling than at Pt-Au tunneling. However, because W-W scanning in air caused tip wear, we conclude that in air the tip-specimen distance was so small that the naturally adsorbed water layers on the tip and specimen were in contact and caused tunnelling barriers of Φ<0.1 eV, just as measured at minimum tip-specimen distance by W-W tunnelling in water, Figure 2c. In Figure 1 the peak-to-peak oscillation of the tip used for spectroscopy was only 0.14 nm, i.e. half the diameter of the water molecule, and with radial transfer of charge to/from the sharp tip, a low tunneling barrier signal is to be expected.

Comparing the relatively *uniform values* of the tunneling barrier signals observed at a surface element of a W-specimen submerged in water and its *topographic smoothness*, Figure 1A, with the *notably lowe*r values of the tunneling barrier signals at the drained surface and its *topographic roughness* in Figure 1B, we have evidence that when submerged, the surface recorded is smoothed by the presence of voids, located at concave solid surface structures. The orderly molecular water structure at void surfaces, caused by the molecular asymmetry at the gas-liquid interface, is assumed to be responsible for their electrical properties being similar to interfacial water at solid surfaces, and thus also the tunneling barrier signals are similar to those

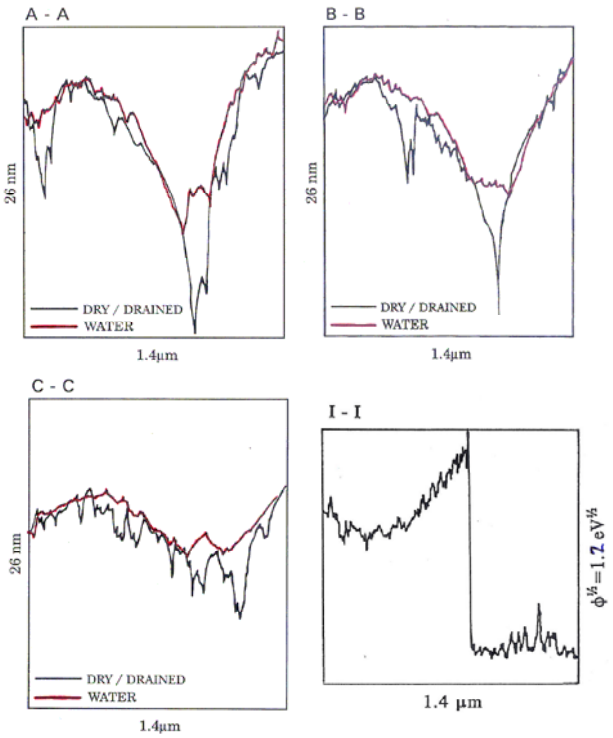

Figure 3. Topographic x-scans A-A, B-B, C-C of a W specimen surface recorded by STM with a W tip, first in water and subsequently when the surface was drained. I-I shows the tunnelling barrier signal in a cross section perpendicular to the scan direction as the tip moved in the y-direction from submerged to drained specimen surface [7].

at attached water. This allows the tip to record the void surface instead of the drained surface beneath it. If at first the tip remained in contact with the drained solid surface below the void, charge transfer would occur along the void surface as well as the drained surface, and the set-point current $I_{t,0}$ would make the tip retract. This explains that STM allows the recording of voids.

Three cross sections of the surface of a W-specimen, A-A, B-B and C-C are shown in Figure 3 with the specimen being first submerged in water, and subsequently drained [7]. The draining of a submerged surface from water (or the covering of a drained surface) caused tip displacements of about 0.1 µm, but characteristic features of the surface being investigated usually allowed it to be relocated by adjustment of the (x,y)-offset voltages [3]. From Figure 3 we get a clear impression of the presence of voids in troughs on the surface, even if we assume that locally, the narrow, cusped canyon bottoms of the drained specimen surface are artifacts, probably the result of tip-specimen contact at locations where the adsorbed water coverage has been insufficient for carrying the pre-set tunneling current. The section I-I shows the shift of the tunneling barrier signal when the tip in successive scans moves from submerged to drained surface positions across the rim of a drop of water on the surface investigated. The signal noise at topographic recordings in water gives a measure of the mechanical and electrical stability of the STM equipment used. On the drained surfaces we can expect an increased uncertainty related to imperfections in the adsorbed layer of water remaining on the surface and allowing the charge transfer demanded, but the systematic and reproducible differences of surface structure observed on submerged and drained surfaces undoubtedly represent the presence of interfacial voids at concave structures of the solid surface.

In addition to revealing the presence of interfacial voids, a major outcome of the STM measurements is the observation of remarkable electrical properties of interfacial water layers. These layers hold the key to explaining the detachment of water from concave surface elements as well as the sharp decline of the tensile strength of water when the temperature of water drops towards the freezing point [8].

However, STM is not an optimal technique for the recording of voids on solid surfaces because the attractive force between tip and void surface make it is difficult to estimate the influence of the tip on the compliant void shape. This force is considered in relation to atomic force microscopy. Further, drained surfaces of normal, oxidized materials may be difficult to record satisfactorily. Finally, in water the Faradayic current has to be eliminated by proper choice of the tip-specimen bias voltage or, preferably, by the use of electrolytic STM. As we shall see, in particular tapping mode atomic force microscopy offers an alternative technique.

Atomic force microscopy

In the atomic force microscope a tiny, sharp conical tip is mounted beneath the end of an elastic cantilever that is fixed to a base block. The base block is positioned by piezo-electric ceramics, basically as the tip holder in a STM. At tip-specimen interaction deflection of the cantilever is recorded optically.

AFM-tips are usually produced by etching technique, and are made from either Si_3N_4 with a cone half-angle of $\alpha \sim 35^o$ and a nominal tip radius of 20-60 nm, or from silicon with $\alpha \sim 15^o$ and a nominal tip radius of <10 nm, Figure 4.

In *contact mode* AFM on a solid surface, a small pre-set upwards (positive) deflection of the cantilever that carries the tip is obtained by tip-surface contact, Figure 5a, and during scanning of the surface the pre-set deflection is maintained by vertical adjustments of the position of the cantilever base block, which thus reflects changes of the surface topography of the specimen.

The topographic recording of a void surface by contact mode AFM demands that at contact it can produce the required upward deflection of the cantilever. This depends on the cone angle of the tip and on the degree of hydrophilicity of the tip surface. With a Si_3N_4 tip submerged in water, the high value of the tip half angle and its limited hydrophilicity cause the tip to be sucked into the void by the *downwards* directed surface tension force F_{st} at contact with the void surface, Figure 4a, and the tip penetrates the void surface until the negative cantilever deflection is able to balance the surface tension forces or ultimately, until contact with the solid surface beneath it is established, Figure 5b. Thus, a large snap-in (>5-10nm) occurring when a Si_3N_4 tip approaches a surface indicates the presence of a void. However, with a Si_3N_4 tip, the void shape cannot be recorded by contact mode AFM, because when the tip meets the void during scanning of the specimen surface, it remains in contact with the solid surface [9].

Conversely, when in contact mode AFM a submerged slender, pointed and highly hydrophilic silicon tip meets an interfacial void during scanning, it is exposed to a surface tension force F_{st} in an *upward* direction when the void surface is penetrated, Figure 4b. If a very small scanning force is

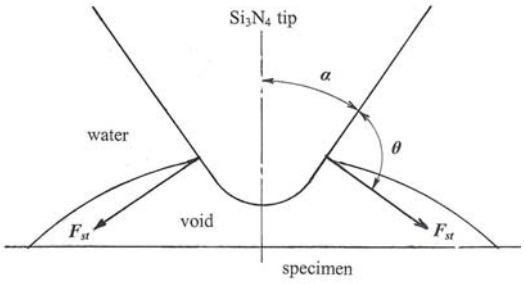

(a)

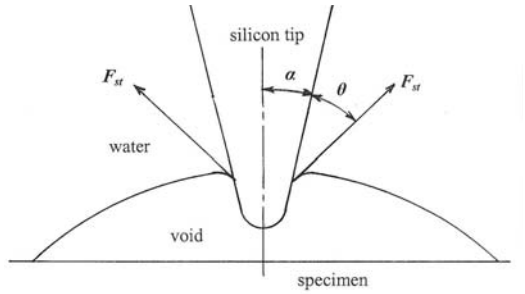

(b)

Figure 4. Surface tension force F_{st} a) on a Si_3N_4 tip, and b) on a silicon tip.

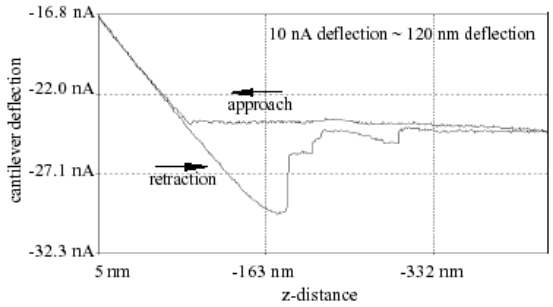

a) AFM-spectroscopy (force curve) at a water-stainless steel interface obtained with a stationary tip-cantilever during its approach and retraction from the specimen surface.

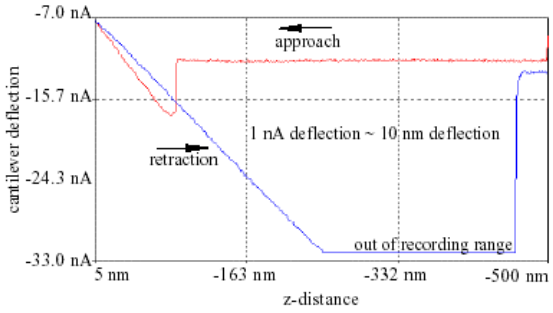

b) AFM-spectroscopy at a void on water-stainless steel interface

Figure 5. At tip approach by contact mode AFM in water a) a snap-in of only a few nm occurs (at $z \approx -87$ nm) when the interfacial layers of orderly structured water on the Si_3N_4 tip and the stainless steel surface merge, while b) an interfacial void causes a snap-in corresponding to the void height/depth (here ~60 nm at $z \approx -87$ nm). At tip retraction a) detachment of the tip begins when the van der Waals forces between tip and specimen are overcome by the cantilever deflection force ($z \approx -150$ nm), while b) at a void also large surface tension forces on the tip have to be overcome ($z \approx -455$ nm) [9].

chosen, this upward surface tension force may produce the positive cantilever deflection demanded for the recording of void surfaces, as obtained in Figure 6a. Here white spots that disappear, and coloured areas that turn darker at an increase of the scanning force, Figure 6b, are voids into which the tip penetrates fully or at least deeper at increase of the force [10,11]. We notice that force balance cannot be obtained until the tip apex itself has penetrated at least partly into the void because $\alpha+\theta$ has to be larger than $\pi/2$. The tip penetration will continue until the contact line of the tip with the bubble surface has grown to give force balance, Figure 4b. Therefore, the bubble heights of 1-1.5 nm recorded in Figure 6 [10,11] are certainly too small. The undisturbed nanobubble heights cannot be determined without full knowledge of the data of the specific tip used – and such data are always difficult to get. The size of the tip apex gives a lower limit for the size of voids that can be recorded in contact mode AFM.

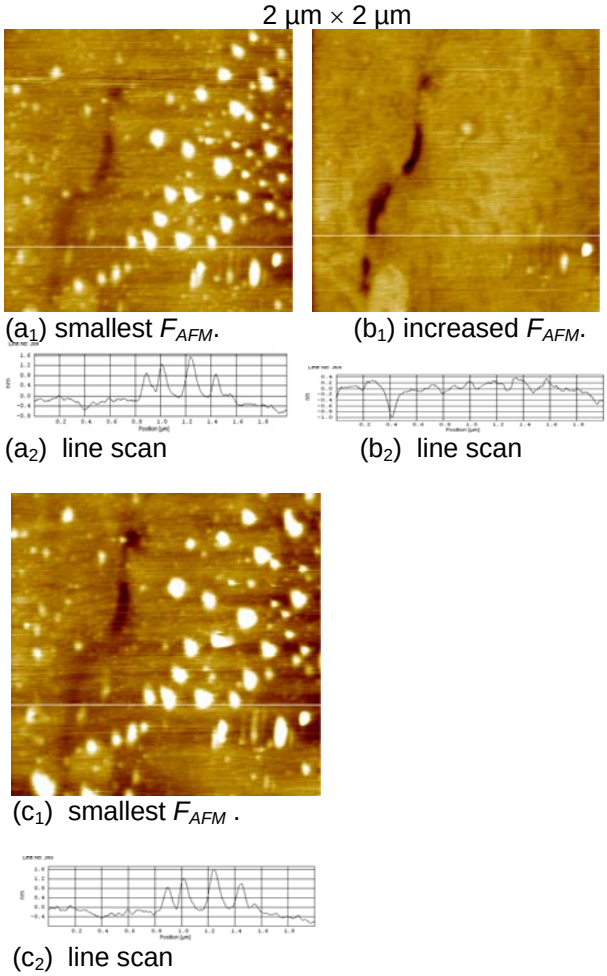

Figure 6. AFM image of a 2 µm × 2 µm gold specimen surface submerged in water and scanned in contact mode with a silicon tip. In (a_1) the smallest scanning force possible is used. (a_2) shows the scan line indicated in (a_1). Subsequently, in (b_1) the specimen is scanned with an increased (a normal) scanning force. (b_2) shows the scan line indicated in (b_1). In (c_1) the smallest possible scanning force is again used. (c_2) is the scan line indicated in (c_1). The white spots are surface nanobubbles. The nanobubbles are penetrated at increase of F_{AFM}. Likewise, the void surface of a gas filled canyon between two single-crystals is penetrated at increase of F_{AFM}. At decrease of the scanning force the voids re-appear, essentially as first observed [10].

Finally we consider *tapping mode* AFM for the recording of surface topography. By this technique the base block carrying the tip-and-cantilever performs vertical vibrations at a frequency very close to the resonance frequency of the tip-cantilever system when positioned off the surface being investigated (~100 kHz for tapping mode tips in air, and a factor of ~5 lower in water). The resonance frequency is highly sensitive to even tiny forces acting on the tip. Therefore, if during the tip oscillation it comes near to a *solid surface*, the van der Waals forces between tip and specimen change both the amplitude of the tip vibration and its phase relative to the driving force of vibration. A pre-set reduction of amplitude is used to govern the z-position of the base block during horizontal scanning, and thus, the surface topography can be identified. This can be achieved even without getting material contact between tip and specimen.

When a solid specimen and the tip are *submerged in water*, the water molecules in direct contact with the tip and specimen surfaces screen the van der Walls forces between them. However, at a tip-specimen distance of a few nm the ordering effects of the solid-like interfacial water layers on the tip and specimen merge, and a similar, though weaker attractive force is set up. In contact mode AFM such interaction causes a weak snap-in, the tip abruptly moves into tip-specimen contact, Figure 5a, but in tapping mode AFM the interaction is sensed when the tip is at its maximum negative cantilever deflection, and the dynamics of the vibrating tip-cantilever system prevents a more than temporary interaction – then the tip again moves away from the solid surface. However, a phase shift and a reduction of the amplitude of tip oscillations are produced. A pre-set reduction of amplitude, the set-point, is used for governing z-displacements of the base block during (x,y)-scanning and so, these record the surface topography. Because water at a *void surface* is also orderly structured, though less than at a solid surface, an attractive force is set up also when the tip approaches a void surface. Therefore, tapping mode AFM actually allows the recording of bubble surfaces when a small amplitude reduction, a high set-point, is chosen for topography detection, [12,13]. However, if the set-point is chosen too high, the tip may loose contact with the surface being investigated.

Using tapping mode AFM, Holmberg [13] shows the presence of nanobubbles on a gold surface. They are imaged topographically, Figure 7a, as well as in phase imaging, Figure 7b. In Figure 7c one of the medium size bubbles is shown as profiles in phase and topography line scans. It is apparent that in phase imaging the bubble diameters appear larger than in topographic imaging. Holmberg considers the phase image to reveal the correct bubble diameter and explains the difference between the topographic and phase images on the assumption that close to the bubble rim the tip penetrates the bubble surface and continues tapping the solid surface until a sufficient bubble height is achieved. This suggests that a sharp *silicon tip* was used[*], and that the set-point chosen has been unable to make the AFM respond to the initial attractive interaction of the very small tip apex with the bubble surface. Therefore the tip has penetrated the bubble surface and reached the solid surface in each tapping motion until at sufficient bubble height, the upward force on the slender cone of the tip, supplied by the bubble surface-tip interaction (Figure 4b), was sufficient to make the AFM respond. The observed decrease of the phase lag at the bubble rim may be ascribed to changes of the tip interaction with the surface beneath it when the bubble rim was passed, and the subsequent increase may be ascribed to the upwardly directed surface tension force on the tip. After horizontal passage of the void rim, this force has gradually

[*] Dr. Holmberg usually used soft contact mode silicon tips for tapping mode AFM in water, presumably also in the present case.

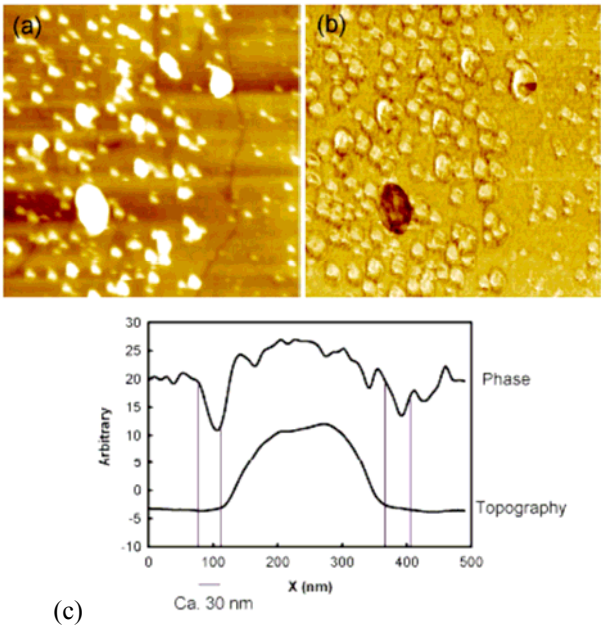

Figure 7. a) Topographic image, and b) phase image of a 5μm×5μm area with nanobubbles on a Au surface, recorded by tapping mode AFM. c) Phase and topographic profiles of a medium size bubble. Courtesy M. Holmberg [13].

weakened the tip-solid surface interaction, and eventually it has broken the contact. Thus, the topographic recordings of bubble diameters and heights become notably affected by the choice of set-point for the AFM, and the bubble dimensions revealed are smaller than those of the real bubbles, while the phase profiles determine the bubble diameters well – as concluded by Holmberg. The asymmetry of the scans in Figure 7c may be ascribed to the use of an inclination of ~10° of the tip-cantilever system relative to the specimen surface.

If, instead of a silicon tip a *Si_3N_4 tip*[♣] is used for tapping mode recording of interfacial voids, the interpretation becomes somewhat different. Due to the larger radius of curvature of the Si_3N_4 tip than that of the silicon tip, a notably larger attractive force on the tip is set up at the merging of the water layer on the tip with that on the specimen below, and a set-point high enough to detect this force may be chosen. When during scanning at such high set-point the tip moves horizontally from the solid surface to the void, the tip starts moving away from the solid surface already at the bubble rim, and then the bubble surface is recorded with small distortion only. (At lower set-point, tip penetration of the void surface occurs, and the downwardly directed surface tension force on the tip, illustrated by Figure 4a, makes the tip penetrate the void surface as when a silicon tip is used, but now the surface tension force remains directed downwards).

Let us study in more detail the Si_3N_4 tip by tapping mode AFM at high set-point. In the narrow space of water between a *solid* surface and a vertically vibrating tip, the water moves outwards radially when the tip approaches, and inwards when it

[♣] For tapping mode AFM e.g. Digital Instruments produces Si_3N_4 tips.

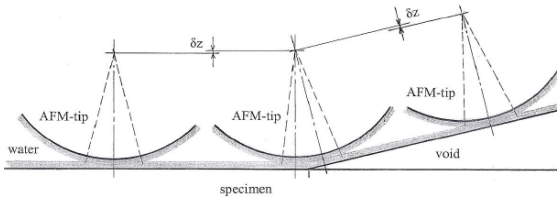

Figure 8. An AFM tip during force interaction at tapping mode operation on a planar solid surface (left), during contact with both the solid surface and the rim of an interfacial nanobubble (middle), and on the bubble surface (right). The grey areas are the water layers affected by the orderly structure of the water at the solid-water and the void–water interfaces. During a small part of the tapping motion of the tip, these layers merge. This causes amplitude and phase shifts that allow detection of solid as well as void surfaces.

retracts from the solid surface. Due to the inertia of the liquid flow, pressure oscillations occur at the tip apex, with a positive optimum at maximum tip-specimen distance, and a negative, but larger optimum at minimum distance, because here the fluid velocities in the radial flow field are larger. This gives a resulting attractive force on the cantilever, which causes an amplitude reduction and a phase lag relative to the driving force of vibration. When the zones of water, affected by the orderly structure of the water adsorbed to the tip and specimen surfaces, start to merge at a tip-specimen distance of some nm, this merging also causes an attractive force that further reduces the amplitude and increases the phase lag. We ignore possible interactions between the two mechanisms. With a set-point close to the initial tip amplitude, we assume that the AFM feed-back system prevents the tip from coming closer than a few nm from the solid surface during its tapping motion. As illustrated in Figure 8 (to the left) it means that for a short time in each cycle of vibration an axisymmetric tip attraction zone exists at the tip apex. With a tip radius R_t=40 nm a radius of merging r_{merge}~10 nm is formed.

We now assume that the vibrating tip scans along a solid surface and meets an attached nanobubble. We choose bubble dimensions from the topographic line scan in Figure 7c: attachment radius Γ_o=125 nm, height of the spherical cap h_o=15 nm, which corresponds to a bubble radius of curvature R_o=530 nm. When during the scanning, the rim of the merging zone at the tip apex approaches the rim of the bubble, the tip starts to interact also with the oblique bubble surface. This causes an increase of the attractive force already before the tip axis reaches the bubble rim, Figure 8 in the middle. However, this increase of force will be compensated by a small tip retraction δz, which reduces the merging zone at the specimen surface. Also the force due to the radial flow between tip and specimen is reduced. The set-point of the feed-back system maintains the amplitude of vibration, but the phase lag is not necessarily unaffected. We notice that now the merging region is not axially symmetrical. At the *bubble surface* the pressure is constant and equal to the gas-vapour pressure inside the bubble. The water between the tip and the bubble wall therefore tends to follow the vertical tip motion instead of performing a radial flow, while in the neighbouring region between the tip and the

solid surface, an oscillating flow and pressure field remains – i.e. a horizontal force now acts on the tip. This indicates that a very small topographic surface rise and a phase shift may be measured already outside the bubble rim. When the tip axis has passed the bubble rim, Figure 8 to the right, we can expect that a new symmetry is established at the tip apex, now with the force on the tip being set up solely by the merging of the water layers at the bubble surface and the tip apex. The attractive force during the tapping motion of the tip may cause surface waves on the void surface, and the attractive force may locally increase the bubble height slightly. Thus, with a Si_3N_4 tip at a set-point close to the undisturbed tip oscillation, we can expect that the topographic image of the bubble surface is only slightly affected by the tip, while due to the bluntness of the tip the diameter in the phase image appears a little larger. At reduction of the set-point the picture at first approaches that obtained with a sharp silicon tip, but ultimately, the void is not recorded because the downward directed surface tension force on the Si_3N_4 tip grows as the height of the void increases towards the center.

CONCLUSION

Experiments have shown that interfacial cavitation nuclei can be recorded by scanning tunnelling microscopy as well as by both contact mode and tapping mode atomic force microscopy. By STM the orderly structured interfacial water layers at the bubble surfaces and on the surfaces of oxidized tips and specimens are decisive for charge transfer to the location of tunnelling. In AFM, these layers produce attractive forces on the tip that allow topographic recording of bubble surfaces.

We can expect that by *STM* in water the orderly structured, solid-like interfacial water layers on the tip and at a bubble surface are separated by liquid-like water that allows a bubble surface to be recorded, but probably with a distortion because the bubble surface is attracted to the tip by the orderly structured liquid layers in the tunnelling gap. Thus, the bubble heights are recorded higher than the real ones.

In *contact mode AFM* it is possible to achieve a force balance between the tip-cantilever system and the bubble surface when *silicon* tips are used, but normally it causes considerable reduction of the bubble height due to penetration of the tip into the void. The recording of voids smaller than the dimensions of the tip apex is not possible. In contrast, we can expect that in *tapping mode AFM* a small bubble distortion can be achieved by using the highest possible set-point (small amplitude reduction) for the AFM. By this technique the tip is in force contact with the bubble surface only during a small part of the cycle of tip vibration. Both Si and Si_3N_4 tips can be used, but it is important for the interpretation of the surface scans, which kind of tip has been used. Systematic studies of interfacial voids by tapping mode AFM using different tips at varied set-points would be most welcome, and topographic as well as phase scans should be studied.

The central role of interfacial water points to the significance of the early studies of "vicinal water" made by Drost-Hansen [14].

Acknowledgments

The author wishes to thank Dr. Maria Holmberg, DTU Nanotech and Drs. Jørgen Garnæs and Kai Dirscherl, Danish Fundamental Metrology for valuable discussions in relation to atomic force microscopy studies. Figure 3 was produced by Prof. Jian Ping Song during his employment at Danish Fundamental Metrology and collaboration with the author in the early 1990'es. Unfortunately this figure was not made available in a journal already at that time. The author gratefully acknowledges the fruitful collaboration with Prof. Song.

NOMENCLATURE

h_o – height of spherical cap
r – radius of merging zone
s – tip-specimen distance
x – scan direction
y – direction in the surface plane $\perp x$
z – direction of the surface normal
F_{AFM} – scanning force
F_{st} – surface tension force
I_t – tunneling current
$I_{t,0}$ – tunneling current at the set-point chosen
R_o – radius of curvature of bubble surface
α – half angle of AFM or STM tip cone
θ – gas-liquid-solid contact angle
Γ_o – radius of attachment of bubble
Φ – tunneling barrier

REFERENCES

[1] Bonnell, D. A. ed. 1993, *Scanning Tunneling Microscopy and Spectroscopy*. VCH Publishers, Inc.

[2] K. A. Mørch, K. A., and Song, J. P. 1992 "Cavitation nuclei at solid-liquid interfaces", *Cavitation – Proc. Institution of Mechanical Engineers*, Int. Conf. Cambridge, UK, Paper C453/059.

[3] Song, J. P., Mørch, K. A., Carneiro, K., and Thölén, A.R. 1993, "STM investigations of solid surfaces in water and air", *Surface Science*, 296**,** 299-309.

[4] Song, J. P., Mørch, K. A., Carneiro, K., and Thölén, A.R. 1994, "Investigation of scanning tunneling barrier signals in air and water", *J. Vacuum Science and Technology* B, 12(3), 2237-2242.

[5] Harvey, E. N., Barnes, D. K., Mc Elroy, W. D., Whiteley, A. H., Peace, D. C., and Cooper, K. W. 1944, "Bubble Formation in Animals", *J. Cellular and Comparative Physiology*, 24, 1-22.

[6] Xia, X., Perera, L., Essmann, U., and Berkowitz, M. L. 1995, "The Structure of Water at Platinum/Water Interfaces, Molecular Dynamics Computer Simulations", *Surface Science*, 335, 401-415.

[7] Mørch, K. A., and Song, J. P. 1993, "STM for Investigation of Cavitation Nuclei in Liquids", *International Conference on Scanning Tunneling Microscopy, STM'93***,** Beijing, August 9-13. Paper OR/TI01.

[8] Mørch, K. A. 2007, "Reflections on cavitation nuclei in water", *Physics of Fluids*, 19, 072104.

[9] Mortensen, N. A., Kühle, A., and Mørch, K. A. 1998, “Interfacial tension in water at solid surfaces”, *Third International Symposium on Cavitation,* Grenoble, France, April 1998, 1, 87-91.

[10] Holmberg, M., Kühle, A., Garnæs, J., Boisen, A., and Mørch, K. A. 2003, ”Cavitation nuclei at water-gold interfaces”, *Fifth International Symposium on Cavitation*, Osaka, Japan, November 2003, Cav03-GS-1-001.

[11] Holmberg, M., Kühle, A., Garnæs, J., Mørch, K. A., and Boisen, A. 2003, “Nanobubble Trouble on Gold Surfaces”, *Langmuir*, 19: 10510-10513.

[12] Lou, S.-T., Ouyang, Z.-Q. Zhang, Y., Li, X.-J., Hu, J., Li, M.-Q., and Yang, F.-J. 2000, “Nanobubbles on solid surfaces imaged by atomic force microscopy”, *J. Vacuum Science and Technology* B, 18(5), 2573-2575.

[13] Holmberg, M. 2003, “Organic and Biological Molecular Layers on Functionalysed Sensor Surfaces Studied with Atomic Force Microscopy”, Ph.D. Thesis, December 2003, Danish Fundamental Metrology, Dept. of Micro- and Nanotechnology, Technical University of Denmark.

[14] Drost-Hansen, W. 1969, “Structure of water near solid interfaces”, *Industrial and Engineering Chemistry*, 61(11), 10-47.